Drug Development and Industrial Pharmacy, 2010; 36(4): 439–448

informa
healthcare

ORIGINAL ARTICLE

Folate-mediated solid–liquid lipid nanoparticles for paclitaxel-coated poly(ethylene glycol)

Lifang Wu[1,2], Cui Tang[1] and Chunhua Yin[1,2]

[1]*State Key Laboratory of Genetic Engineering, School of Life Sciences, Fudan University, Shanghai, China and* [2]*Department of Biochemistry, School of Life Sciences, Fudan University, Shanghai, China*

Abstract

Background: As a promising anticancer drug, severe side-effects of current clinical formulations for paclitaxel have restricted its use, developing a better technical-economical formulation for paclitaxel delivery is needed. *Method*: In this study, the compound of folate-poly(ethylene glycol) (PEG)-phosphatidylethanolamine was synthesized and characterized with Fourier transform infrared spectroscopy and nuclear magnetic resonance spectroscopy. The solid-liquid lipid nanoparticle (SLLN) for paclitaxel modified with folate and poly(ethylene glycol) (folate-PEG-SLLN) was prepared and characterized. Morphology of folate-PEG-SLLN was examined by transmission electron microscopy. The particle size and zeta potential were performed by Zetapals. Encapsulation efficiency was analyzed by HPLC. The in vitro drug release of paclitaxel was investigated via membrane dialysis. The in vivo pharmacokinetics was measured with male Sprague-Dawley rats. Treatment efficiency was investigated with the mouse with sarcoma180 ascites tumor. *Results*: Paclitaxel loaded on the newly designed binary SLLN showed a longer and sustained in vitro releasing property. More importantly, S180 tumor-bearing mice treated with paclitaxel-loaded SLLN exhibited higher tumor inhibition rate, comparing with animals administered with paclitaxel injection alone (45.3% and 37.3%, respectively). *Conclusion*: The newly developed paclitaxel delivery system may have improved in vivo antitumor activity. The results demonstrated a great interest to use folate-mediated SLLN as a prospective drug delivery system for paclitaxel.

Key words: *Drug delivery system; folate; paclitaxel; pharmacokinetics; solid–liquid lipid nanoparticles; tumor inhibition rate*

Introduction

Paclitaxel, as a promising anti-cancer drug candidate, has exhibited widespread and significant anti-solid tumor activities[1–4]. However, the low water solubility of paclitaxel, which is 0.30 μg/mL at 37°C[5], has restricted the efficient development of paclitaxel formulations. Currently, paclitaxel formulated in a 1:1 mixture of Cremophor® EL (polyethoxylated castor oil) with ethanol as the commercially available product named Taxol®[6,7] has been widely used as an FDA-approved anti-cancer drug. However, Taxol® has limited stability after dilution. Moreover, Cremophor® EL could cause severe in vivo hypersensitivity reactions[8,9]. Therefore, more effective formulations of paclitaxel with less severe in vivo toxicity need to be developed[10]. More recently, a new formulation product named ABI-007 (Abraxane®; Abraxis Bioscience Inc., Los Angeles, CA, USA) has been approved for breast cancer treatment[11,12]. Abraxane® is an albumin-bound particle form of paclitaxel, which presents greater efficacy and more favorable safety profile compared to Taxol®[11,12]. Because of the high cost and limited resource of human albumin used in the particle, it is necessary to develop a better technical-economical formulation for paclitaxel delivery.

Solid lipid nanoparticles gain great popularity because of their multiple favorable features, including their potentially broader applications, introducing biodegradable physiological lipids, producing nonorganic solvents, with the potential to scale up for industrial production and for site-specific targeting[13,14]. However, the drug loading capacity of conventional solid lipid

Address for correspondence: Dr. Lifang Wu and Professor Chunhua Yin, State Key Laboratory of Genetic Engineering, School of Life Sciences, Fudan University, Shanghai 200433, China. Tel: +86 21 6564 3797, Fax: +86 21 5552 2771. E-mail: wlfang2008@sina.com; chyin@fudan.edu.cn.

(Received 8 Jun 2009; accepted 5 Aug 2009)

ISSN 0363-9045 print/ISSN 1520-5762 online © Informa UK, Ltd.
DOI: 10.3109/03639040903244472

nanoparticle is less than 50%[15]. The combination of solid lipids and liquid oils was proposed to increase drug loading efficiency[16]. Nevertheless, the efficiency of current complex drug delivery system is still limited by its short circulation time and nonspecific in vivo targeting.

To obtain long-circulating drug carriers, the surface of nanoparticless can be coated with flexible hydrophilic polymers such as poly(ethylene glycol) (PEG), which prolongs its half-life in blood to some extent[17], and spontaneously accumulates in solid tumors via enhanced permeability and retention effect through its passive targeting mechanism[18].

Folic acid (folate) (FA) as a ligand specifically targeted to cancer cells could be employed for cancer-specific targeting. Folate receptor (FR) has been identified as a useful tumor marker as the expression and cell membrane localization of FR on tumor cells are significantly higher than on normal cells[19–22]. As a high-affinity ligand for the FR (K_d ~ 0.1 nM), folate combined with drug delivery system could achieve tumor tissue-specific drug targeting based on the specific interaction between folate and receptors[23–26]. The development of tumor-specific targeting delivery of anti-cancer drugs, proteins, and genes via a FR-mediated endocytosis system has been broadly reported[27–30], although the in vivo evaluation, especially therapeutic efficacy of this system, is not well-studied.

In this study, the derivative, namely folate-PEG–phosphatidylethanolamine (PE), was synthesized and incorporated into solid–liquid lipid nanoparticles (SLLN). Moreover, the SLLN modified with folate and PEG for paclitaxel delivery (folate-PEG–SLLN) were further characterized and functionally evaluated in vivo. The pharmacokinetic behavior and anti-tumor efficiency of the folate-PEG-SLLN were also studied in rats and S-180 tumor bearing mice, respectively, which were compared with Cremophor® EL formulation of paclitaxel.

Materials and methods

Materials

Paclitaxel was purchased from Shanghai Hualian Pharmaceutical Co., Ltd. (Shanghai, China). Cremophor® EL was a gift from BASF Corporation. Dynasan118 (tristearin glyceride) was purchased from Shanghai No. 1 Chemical Plant (Shanghai, China). Soybean lecithin (L-α-phospatidylcholine) of medicinal grade was purchased from Shanghai No. 1 Oils and Fats Factory (Shanghai, China). Miglyol 812N (caprylic/capric triglycerides) was gifted by Sasol Company (Johannesburg, South Africa). PEG–PE (M.W.2,250), L-α-PE, polyoxyethylene-bis-amine (H_2N-PEG-NH_2, M.W.3,350), dicyclohexylcarbodiimide (DCCI), *N*-hydroxysuccinimide, FA, succinic anhydride, and sorbitan monostearate (Span60) were all purchased from Sigma Chemical Co. (St. Louis, MO, USA). Sephadex G-75 and G-25 were obtained from Pharmacia (Peapack, NJ, USA). Acetonitrile (Merck, Germany) was of high-performance liquid chromatography (HPLC) grade. All other chemicals were of analytical grade and were used without further purification.

Synthesis of folate-PEG–PE and preparation of folate-PEG–SLLN

Folate-PEG–PE was synthesized as reported by Lee in 1995[25] with some modifications. In brief, 500 mg polyoxyethylene-bis-amine and equimolar quantity of FA were added to 5 mL dimethylsulfoxide containing one molar equivalent of DCCI and 125 μL triethylamine. The reaction mixture was stirred in the dark at 30°C for 24 hours. Then adding 10 mL water into it and removing the by-product, dicyclohexylurea, by centrifugation. The supernatant was dialyzed against water. The dialyzed supernatant was lyophilized to produce folate-PEG–NH_2. After that, *N*-succinyl PE was synthesized by mixing the following chemicals: 1.0 g PE in 50 mL chloroform containing 50 μL triethylamine and equimolar amount of succinic anhydride. The reaction occurred at 30°C for 24 hours. After 24 hours, the reaction mixture was concentrated under reduced pressure and the product was precipitated with cold acetone. Following precipitation, *N*-succinyl PE was redissolved in chloroform and reacted with equimolar DCCI at 30°C for 4 hours to activate its carboxyl group. In this reaction mixture, an equimolar quantity of the above synthesized folate-PEG–NH_2 dissolved in chloroform was added. The reaction mixture was stirred at room temperature for 24 hours, then concentrated under reduced pressure, and the product was precipitated with cold diethylether. The coarse product was further purified by Sephadex G-25 gel filtration chromatography. Isocratic elution was performed using 100 mmol/L (pH 8.0) ammonium acetate at a flow rate of 100 μL/min. The UV detector was set at 280 nm. The first elution product was collected and dialyzed to remove the salt in the eluant. Then the dialysate was lyophilized. The product was confirmed by Fourier transform infrared spectroscopy and nuclear magnetic resonance (^{1}H-NMR).

Folate-PEG–SLLN was prepared as follows. Briefly 2 mL ethanol solution consisting of 100 mg lecithin was blended with 5 mL mixture solution in acetone that contains 10 mg paclitaxel, 200 mg Dynasan 118, and 100 μL Miglyol 812 N. The said mixture was added to 30 mL water solution containing 200 mg folate-PEG–PE, followed by stirring at 70 ± 2°C for 4 hours before acetone was removed. Then the suspension was quickly dispersed to

60 mL of water at 0–2°C and solidified for 2 hours. The product was called folate-PEG–SLLN. The SLLN prepared with emulsifier Span60 (without PEG chain) or PEG–PE was designated as Span60–SLLN or PEG–SLLN, respectively. Each SLLN was performed in triplicate.

Physicochemical characterization of paclitaxel-loaded folate-PEG–SLLN

Morphology of folate-PEG–SLLN was examined by transmission electron microscopy (JEM-1200EX; JEOL Company, Japan). The particle size and zeta potential were performed by Zetapals (Zetapals, Brookhaven, NY, USA). Samples for zeta potential measurement were diluted with water adjusted to a conductivity of 50 μS/cm using sodium chloride. Measurements were performed in triplicate. Encapsulation efficiency (EE) was analyzed by HPLC. Sephadex G-75 was presoaked with deionized water and packed into a 15 mm × 100 mm column equilibrated with water. The folate-PEG–SLLN suspension of 400 μL was applied to the column and then eluted with water. The elution was collected in 1 mL fractions in vials and thereafter analyzed by laser light scattering to identify the fraction(s) containing nanoparticles. Then, the amount of paclitaxel loaded in nanoparticles was analyzed by HPLC. Another folate-PEG–SLLN suspension of 400 μL was directly dissolved in methanol and centrifuged at 32,000 × *g* for 30 minutes. The amount of paclitaxel in the supernatant was analyzed by HPLC, which represented the original amount of paclitaxel in the folate-PEG–SLLN suspension of 400 μL. Each analysis was performed in triplicate. Drug EE was defined as the ratio of the actual amount of paclitaxel loaded in nanoparticles to the original amount of paclitaxel in folate-PEG–SLLN suspension. The calculation equation is as follows:

$$\text{Encapsulation efficiency (EE)} = \frac{\text{actual amount of paclitaxel loaded in nanoparticles}}{\text{theory amount of paclitaxel loaded in nanoparticles}} \times 100\%.$$

In vitro drug release of paclitaxel-loaded folate-PEG–SLLN

The in vitro drug release of paclitaxel-loaded folate-PEG–SLLN was investigated through membrane dialysis at 37°C. A Spectra/Pro® regenerated cellulose dialysis membrane with the molecular weight cutoff size of 14,000 Da was used; the nanoparticles suspension was dialyzed against pH 7.4 phosphate-buffered saline (PBS) containing 0.1% (w/v) Tween 80. At fixed time intervals, 1 mL of the release medium was replaced by 1 mL of fresh medium. HPLC was used to determine the concentration of paclitaxel, and the percentage of cumulative amount of released paclitaxel was calculated accordingly.

The HPLC system is composed of an LC 10ATvp pump (Shimadzu, Kyoto, Japan), a Rheodyne Model 7725 injection valve equipped with a 20 μL loop (Torrance, CA, USA), an SPD-10A UV–Vis detector (Shimadzu), and an HS 2,000 series of chromatographic workstation (Hangzhou Yingpu Co., Hangzhou, China). The column used was Hypersil C_{18} 150 mm × 4.6 mm (10 μm; Yilite, Dalian, China). The UV detector was set at 227 nm. Isocratic elution was performed using acetonitrile/water (58:42, v/v) with flow rate at 1.0 mL/min.

Pharmacokinetics analysis

Care and handling of animals and animal experiment protocols were approved by Fudan University Animal Care and Use Committee in accordance with NIH Guidelines. The in vivo pharmacokinetics were measured with male Sprague–Dawley rats of 200–240 g, which were supplied by the Laboratory Animals Centre of Fudan University. The animals were housed in air-conditioned facility and provided with standard food and filtered water.

The animals used were randomly assigned to three groups, with three rats in each group. The rats in group 1 were injected with paclitaxel-loaded Span60–SLLN, group 2 with paclitaxel-loaded PEG–SLLN, and group 3 with paclitaxel-loaded folate-PEG–SLLN. Three formulations were administered via the tail vein at the same dose of 6 mg/kg paclitaxel. For all groups, blood samples were collected from the orbital sinus at 0.5, 1, 2, 4, 8, 12, and 24 hours after administration. Plasma samples were harvested by centrifugation at 2,000 × *g* for 10 minutes and stored at −20°C until analysis. Liquid–liquid extraction was performed prior to analysis by HPLC. Briefly, 25 μL of internal standard diazepam (1.0 μg/mL, in methanol) was added to 200 μL of rat plasma and the mixture was extracted with 4 mL of absolute ethyl ether on a vortex-mixer for 2 minutes. After standing for 5 minutes, the organic layer was transferred to a clean tube and evaporated under nitrogen at 40°C. The residue was reconstituted with 100 μL of acetonitrile and then centrifuged at 12,000 rpm for 10 minutes; 20 μL aliquot was injected to HPLC column. HPLC system was the same as the in vitro release evaluation except that the column is Diamonsil-C18 (200 mm × 4.6 mm, 5 μm) added with a guard cartridge (Waters Nova-pack C_{18}). The mobile phase is ammonium acetate (10 mmol/L, pH 5.0)/acetonitrile (54:46, v/v), with flow rate at 1.0 mL/min.

Pharmacokinetic parameters were expressed as area under the curve (AUC), terminal elimination half-life ($t_{1/2}\beta$), mean retention time (MRT), and clearance (CL).

Treatment efficiency

The mouse with sarcoma180 (S-180) ascites tumor was gifted by Laboratory Animals Centre of Shanghai Institutes for Biological Sciences, Chinese Academy of Science. The ascites with S-180 tumor cells were collected and diluted into a single-cell suspension containing 5×10^6 cells/mL. The mice received inoculations of 1×10^6 cells/mouse on day 0 at the right forelimb armpit. The drugs were administered through tail vein on the sixth day after tumor cell inoculation. Tumor-bearing mice were divided into five groups, having eight animals in each group. Group 1 was injected with normal saline (NS). Group 2 with paclitaxel injection (6 mg/kg/day), group 3 with folate-PEG–SLLN (6 mg/kg/day), group 4 with folate-PEG–SLLN (4 mg/kg/day), and group 5 with folate-PEG–SLLN (2 mg/kg/day). Formulations were administered successively for 3 days. Mice were killed on the day 14 after the first drug administration. The tumor was measured in terms of maximum and minimum diameter before isolation and weighing. Tumor volume was calculated according to the following formula: $V = ab^2/2$, (a, maximal diameter of the tumor; b, minimum diameter of the tumor)[31]. Calculation formula of inhibition rate (IR) was as follows: IR = $(1 - W_t/W_c) \times 100\%$, where W_c and W_t were the average tumor weights of the control- and sample-treated groups, respectively[32].

Histopathology and morphological observations

After treating the mice for 14 days with NS, folate-PEG–SLLN (6 mg/kg/day), and paclitaxel injection (6 mg/kg/day) as described above, a portion of tumor was isolated and cut into small pieces, fixed in Heidenhain's Suea Fluid ($HgCl_2$: 4.5 g; NaCl: 0.5 g; distilled water: 80.0 mL; formalin: 20.0 mL; acetic acid: 4.0 mL; trichloroaceticacid: 2.0 mL), and then stained with hematoxylin and eosin (HE), examined, and photographed under an OLYMPUS microscope.

Statistical analysis

All the data were expressed as mean ± SD. Statistical comparisons were performed with Student's t-test. A P-value of less than 0.05 was considered statistically significant.

Results and discussion

Synthesis of folate-PEG–PE

Folate-PEG–PE was synthesized with PEG-bis-NH_2 and PE through two-stepped reactions (Figure 1). The reaction mixture was dealt with anhydrous ethyl ether to precipitate folate-PEG–PE. The coarse product was further purified by Sephadex G-25 gel filtration chromatography, which could separate folate-PEG-NH_2, folate-PEG-folate, and folate-PEG–PE. Thin-layer chromatography of the fraction of folate-PEG–PE displayed a single spot with retention factor (R_f) of 0.85. As shown in Figure 2B, a strong peak appears at 1720 cm^{-1} in the Fourier transform infrared spectroscopy; spectrum of folate-PEG–PE represents the newly formed amide linkage (Figure 2). The peak at 2887 cm^{-1} was the CH_2 group of PEG (Figure 2B).

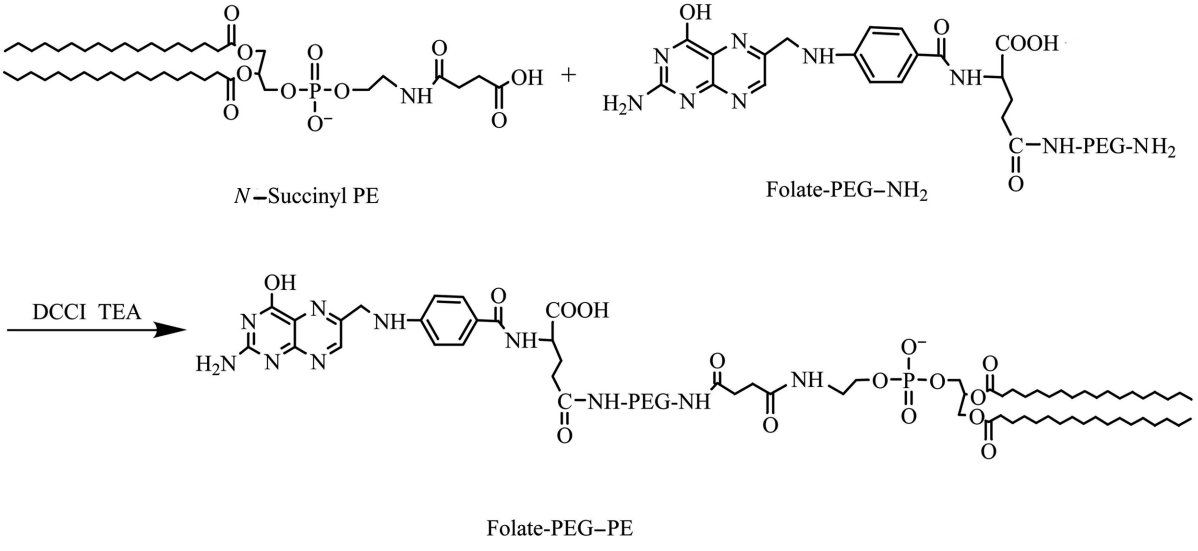

Figure 1. Schematic representation of de novo synthesis of folate-PEG–PE.

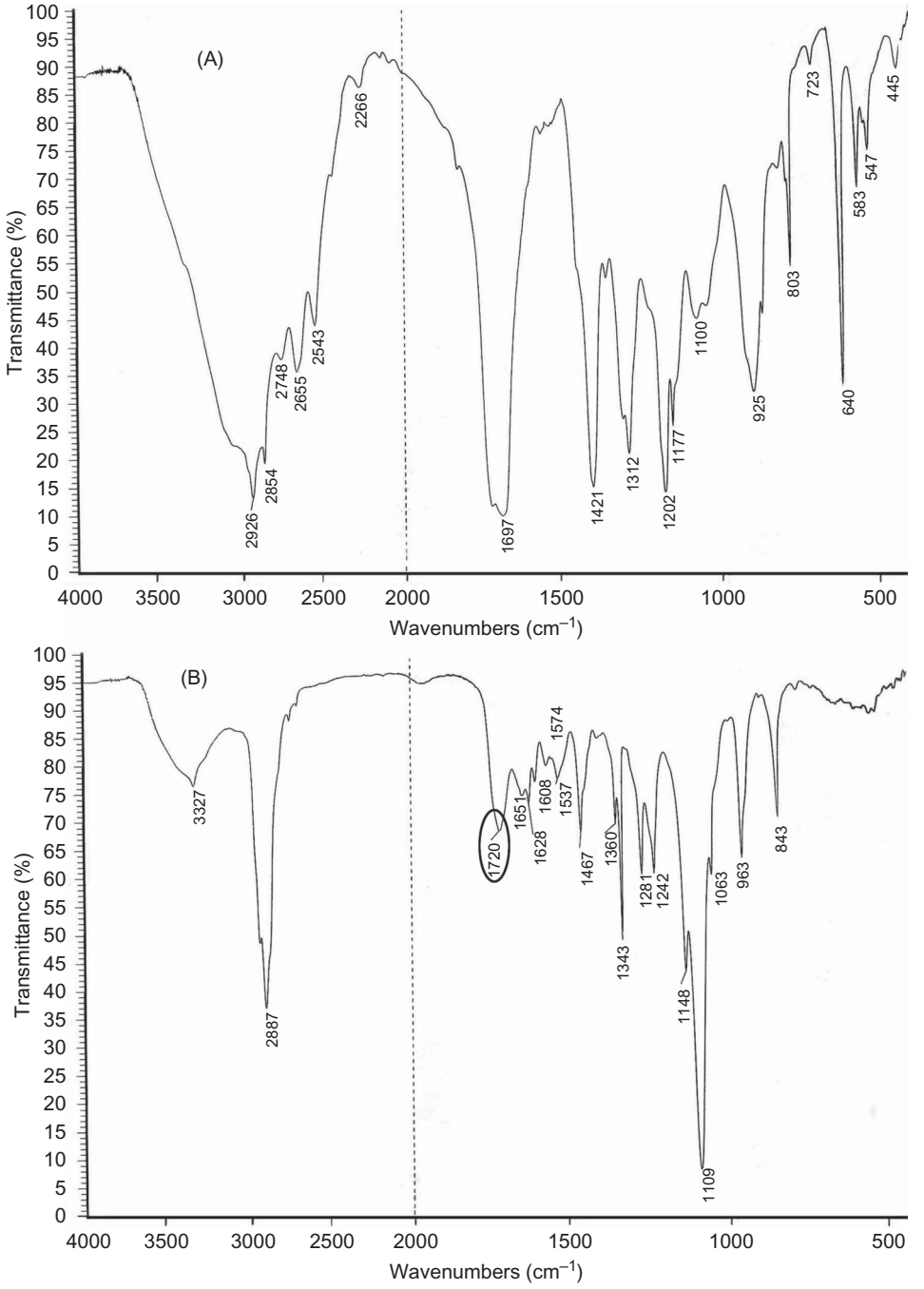

Figure 2. Fourier transform infrared spectroscopy spectra of (A) physical mixture of folate-PEG–NH_2 and *N*-succinyl PE and (B) folate-PEG–PE.

^{1}H-NMR spectroscopy of folate-PEG–PE exhibited chemical shifts at 4.21 and 2.48 ppm, which can be ascribed as α-CH_2, β,γ-CH_2 in glutamate moiety of folate. Moreover, δ = 3.64 ppm was the repeated units of PEG, –OCH_2CH_2 (Figure 3). The result was in accordance with what Liu[33] reported. In summary, folate-PEG–PE has been prepared using the above method with a yield of 7.5% according to PE.

Preparation and characterization of paclitaxel-loaded folate-PEG–SLLN

We prepared folate-PEG–SLLN by the procedure named emulsification at a high temperature and solidification at a low temperature. In brief, folate-PEG–SLLN appeared to be round in shape with good dispersion (Figure 4). Besides, as the arrows showed in Figure 4A,

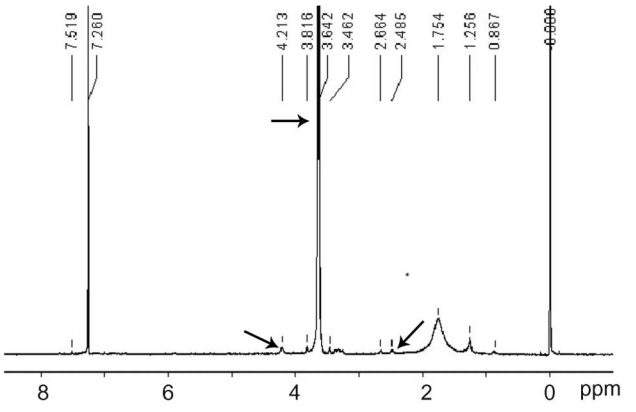

Figure 3. ^{1}H-NMR spectrum of folate-PEG–PE.

we observed the PEG 'shells' on the surface of nanoparticles. The entrapment efficiency of folate-PEG–SLLN was as high as 98%. The mean particle diameter was 207 nm. The zeta potential of folate-PEG–SLLN was –34 mV. As PEG is uncharged, the negative charge should be attributed to the presence of ionized carboxyl groups from stearic acid or caprylic acid on the surface of nanoparticles.

In vitro drug release of paclitaxel-loaded folate-PEG–SLLN

The 0.1% (w/v) Tween 80 was added to PBS with pH 7.4 to increase its solubility and to avoid binding of paclitaxel to the membrane[34]. Figure 5 showed the in vitro release of paclitaxel from paclitaxel injection and folate-PEG–SLLN, respectively. Paclitaxel injection was made in the laboratory according to clinical formulation with a 1:1 mixture of Cremophor® EL and ethanol. Paclitaxel was completely released in 6 hours in solution (Figure 5A), whereas folate-PEG–SLLN was released about 54% in 15 days, and showed a quick initial releasing rate of paclitaxel in the first 2 days while a slow and sustained releasing rate was detected thereafter (Figure 5B). The initial release was probably because of drug molecules bound on the nanoparticles shell while the sustained releasing profile thereafter may be attributed to the paclitaxel molecules entrapped within the nanoparticles oily core. This result may be explained by PEG chain that could effectively prolong the in vitro release time of paclitaxel from the nanoparticles.

Pharmacokinetics study of paclitaxel-loaded folate-PEG–SLLN in rats

Besides the study on the in vitro drug release of paclitaxel, we also performed the pharmacokinetics study of paclitaxel-loaded folate-PEG–SLLN. Figure 6 showed the plasma concentration–time profiles of paclitaxel after intravenous injection of Span60–SLLN, PEG–SLLN, and folate-PEG–SLLN preparations in rats at a paclitaxel dose of 6 mg/kg. At 12 hours post-injection, the paclitaxel concentration in plasma of Span60–SLLN, PEG–SLLN, and folate-PEG–SLLN groups was 113.5, 423.2, and 347.7 ng/mL, respectively. The concentration of paclitaxel in the plasma of rats treated with PEG–SLLN and folate-PEG–SLLN was obviously higher than that treated with Span60–SLLN, which did not contain PEG chains. At 24 hours after administration, the concentration of paclitaxel in the plasma of Span60–SLLN-treated group was undetectable, while for the groups of PEG–SLLN and folate-PEG–SLLN, the paclitaxel concentration in plasma was still 375 and 258.7 ng/mL, respectively (Figure 6). In conclusion, PEG–SLLN and folate-PEG–SLLN showed slower elimination during blood circulation. The desired results may attribute to the

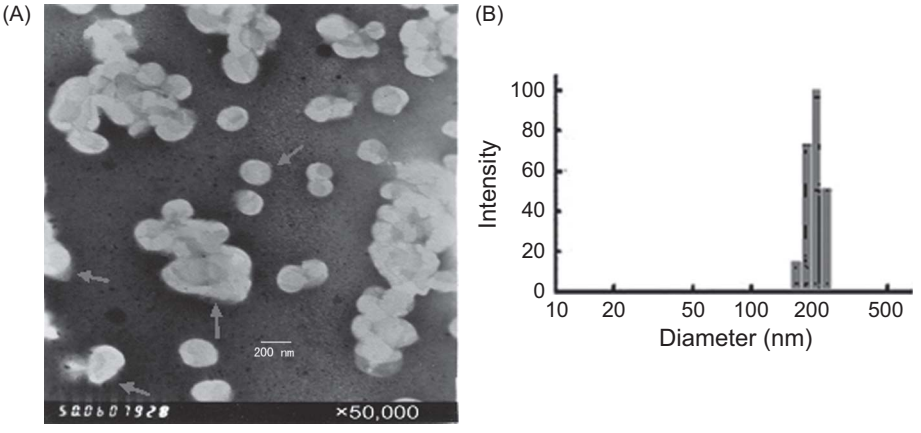

Figure 4. (A) Transmission electron microscopy image of folate-PEG–SLLN. (B) Laser diversity chart for measuring the diameter and distribution of folate-PEG–SLLN.

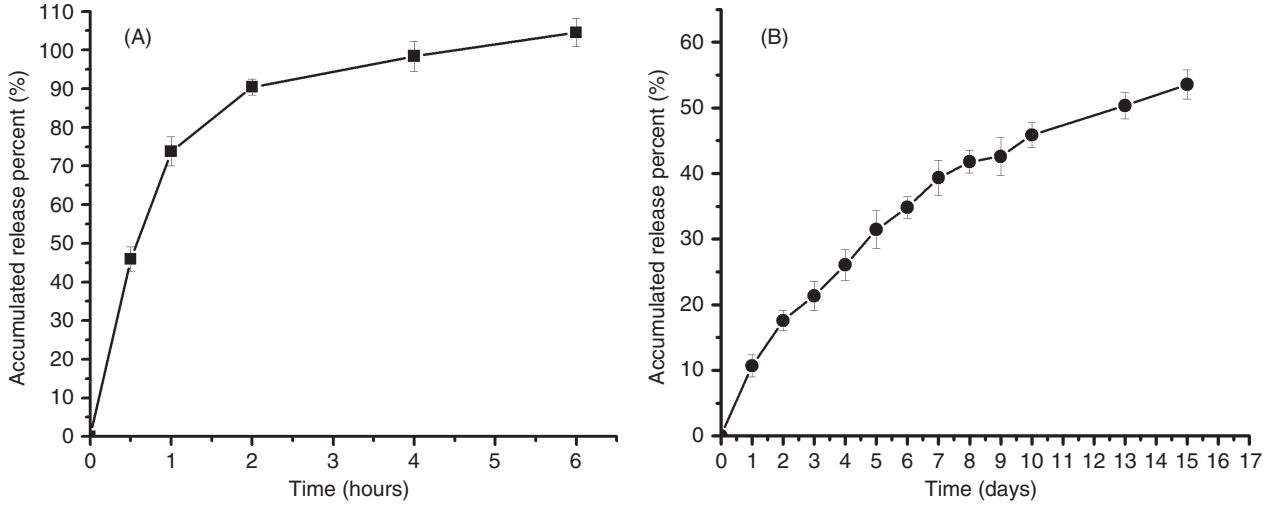

Figure 5. In vitro drug release profiles of paclitaxel-loaded (A) paclitaxel injection and (B) folate-PEG–SLLN in PBS (pH 7.4) containing 0.1% Tween 80. Each point represents the mean ± SD, $n = 3$.

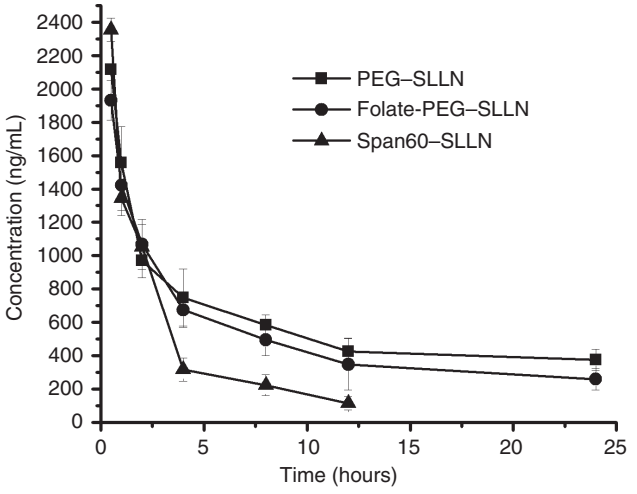

Figure 6. Plasma concentration–time profiles of paclitaxel after intravenous injection to SD rats at 6 mg/kg dose formulated in Span60–SLLN, PEG–SLLN, and folate-PEG–SLLN, respectively. (At 24 hours post-administration, plasma sample of Span60–SLLN was not detected.) Each point represents the mean ± SD, $n = 3$.

hydrophilic polymer PEG, which inhibited protein adsorption and opsonization of nanoparticles and significantly increased half-life of the drug in animal blood. We also summarized pharmacokinetic parameters of the drugs measured in animal blood in Table 1. The MRT and terminal elimination half-life ($t_{1/2}\beta$) of folate-PEG–SLLN significantly increased to 11.46 and 8.38 hours, respectively, compared to 5.82 and 5.41 hours of Span60–SLLN, and only 0.52 and 1.65 hours of Taxol®, respectively[35]. The prolonged MRT and $t_{1/2}\beta$ of folate-PEG–SLLN indicated that folate-PEG–SLLN possessed long-circulating properties with a slow distribution and elimination phase, which may favor to target tumor sites. Compared with Span60–SLLN, folate-PEG–SLLN and PEG–SLLN showed significant difference in MRT, $t_{1/2}\beta$, $AUC_{0-\infty}$, and CL (P = 0.0399, 0.041, 0.0477, 0.0269 and P = 0.0048, 0.0013, 0.0164, 0.0030, respectively). Folate-PEG–SLLN and PEG–SLLN preparations exhibited a similar CL profile, and no statistical difference was observed in the calculated pharmacokinetic parameter for both formulations (P = 0.291, 0.4924, 0.8259, and 0.4565 in $t_{1/2}\beta$, $AUC_{0-\infty}$, CL, and MRT), which suggested that the

Table 1. Pharmacokinetic parameters of paclitaxel after intravenous injection administration of Span60–SLLN, PEG–SLLN, and folate-PEG–SLLN in rats (dose: 6 mg/kg).

	$AUC_{0-\infty}$(ng/hmL)	$t_{1/2}\beta$ (hours)	CL (mL/kg/min)	MRT (hours)
Span60–SLLN	6126.08 ± 445.05	5.41 ± 0.39	979.42 ± 71.15	5.82 ± 0.42
PEG–SLLN	14,509.18 ± 976.09*	9.72 ± 0.65*	413.53 ± 27.81*	13.55 ± 0.91*
Folate-PEG–SLLN	12,046.10 ± 987.19*	8.38 ± 0.68*	498.09 ± 40.81*	11.46 ± 0.93*

AUC, area under the curve; $t_{1/2}\beta$, terminal elimination half-life; MRT, mean retention time; CL, clearance.
*$P < 0.05$ versus Span60–SLLN.

conjugation of FA to PEG terminal did not significantly affect the functional PEG chain.

Tumor inhibition rate of paclitaxel-loaded folate-PEG–SLLN in S-180-bearing mice

The in vivo therapeutic efficacy of folate-PEG–SLLN for paclitaxel was evaluated, based on its ability of inhibiting tumor growth (tumor IR). Descriptive and statistical data from the tumor IR study were presented in Table 2. On the day 14 after first drug administration, only five of total eight mice survived in the NS group and in the 4 mg/kg folate-PEG–SLLN paclitaxel-treated group, only seven of total eight mice survived in the paclitaxel injection-treated group as well as in 6 mg/kg folate-PEG–SLLN paclitaxel-treated group. With regard to the tumor volume, 6 mg/kg folate-PEG–SLLN paclitaxel-treated group showed a statistically significant difference compared with the NS group (P = 0.0274). P-value of paclitaxel injection group was 0.0549 compared with the NS group. However, 6 mg/kg folate-PEG–SLLN paclitaxel-treated group exhibited no significant decrease in tumor volume compared to paclitaxel injection-treated group (P = 0.1812). The tumor IRs of folate-PEG–SLLN and paclitaxel injection group at 6 mg/kg dose were 45.3% and 37.3%, respectively, suggesting significant increase in IR compared to NS group (P = 0.0029 and P = 0.0165, respectively). The results also showed that the IR of folate-PEG–SLLN-treated group was not significantly increased, compared with paclitaxel injection group, suggesting the therapeutic equivalency of both formulations.

Lee and Low reported that uptake of folate-PEG–liposomal DOX by KB cells was 1.6 times higher than that of free DOX[25]. In this study, the IR of paclitaxel-loaded folate-PEG–SLLN-treated group was only 21% higher than paclitaxel injection-treated group. The possible reasons are stated as follows. First of all, in our experiment the mice were fed in ordinary diet, but the cell uptake experiment of Lee was carried out in the FA-free medium; the free FA can competitively combine with FR[36,37]; therefore, more free FA may reduce the binding of folate-PEG–SLLN to FR and decrease the therapeutic efficacy. Second, the expression level of FR in the S-180 tumor cell used in this study is not investigated; while in KB cell, it is overexpressed; therefore, FR of S-180 needs to be further investigated. Third, the difference of the in vivo and the in vitro environment may result in the variance. Zhang observed that folate-mediated albumin nanoparticles showed targeting tumor cell in vitro cell experiment and in vivo biodistribution, though the targeting degree in vivo was obviously less than in vitro[38]. At present, the in vivo study of folate-mediated targeting is still limited, and this calls for further evaluation in the future.

Histopathology and morphological observations

We found that tumors shrunk significantly in folate-PEG–SLLN group ($P < 0.05$) and shrunk less in paclitaxel injection group ($P > 0.05$) compared with NS group (Table 2). The histopathological studies of tumor from the test groups indicated that the tumor cells from the folate-PEG–SLLN and paclitaxel injection-treated groups had nucleus pyknosis and necrosis areas in different degrees (Figure 7A–C). There were many large irregular karyons and polykaryocytes among the tumor cells from the NS-treated groups (Figure 7A). After treated with paclitaxel injection (6 mg/kg·day for 3 days), these tumor cells only decreased a bit (Figure 7C). But treated with folate-PEG–SLLN (6 mg/kg/day for 3 days), the large irregular karyon and polykaryocyte of the tumor cells were decreased significantly and the necrosis areas were obvious (Figure 7B). Therefore, folate-PEG–SLLN may inhibit the growth of tumor cells more effectively than paclitaxel injection at the same dose.

Conclusion

In this study, we demonstrated long-circulating properties of our newly synthesized folate-PEG–SLLN. Moreover, paclitaxel-loaded folate-PEG–SLLN appeared to have higher tumor IR, compared with the current clinically used paclitaxel formulation in a model of S-180, which exhibited an improved therapeutic efficacy of

Table 2. The in vivo anti-tumor efficiency of paclitaxel injection and folate-PEG–SLLN treated in S-180 tumor-bearing mice.

Drug	Dose (mg/kg)	Mice In./Fi.	Body wt. (g) In./Fi.	Tumor volume (cm^3)	Tumor wt. (g)	IR (%)
NS	0	8/5	31.4/48.3	20.1 ± 9.6	11.2 ± 3.3	—
Injection	6	8/7	30.2/40.9	13.5 ± 3.0	7.0 ± 2.5	37.3*
SLLN	6	8/7	29.7/37.5	12.1 ± 2.3*	6.2 ± 1.7	45.3*
	4	8/5	30.2/41.4	18.9 ± 3.4	7.7 ± 2.0	31.4
	2	8/6	29.5/43.9	20.0 ± 5.8	7.7 ± 2.6	31.3

In., day 0 of experiment; Fi., day 20 of experiment; NS, normal saline; solution, paclitaxel injection; SLLN, folate-PEG–SLLN.
*$P < 0.05$ versus NS group.

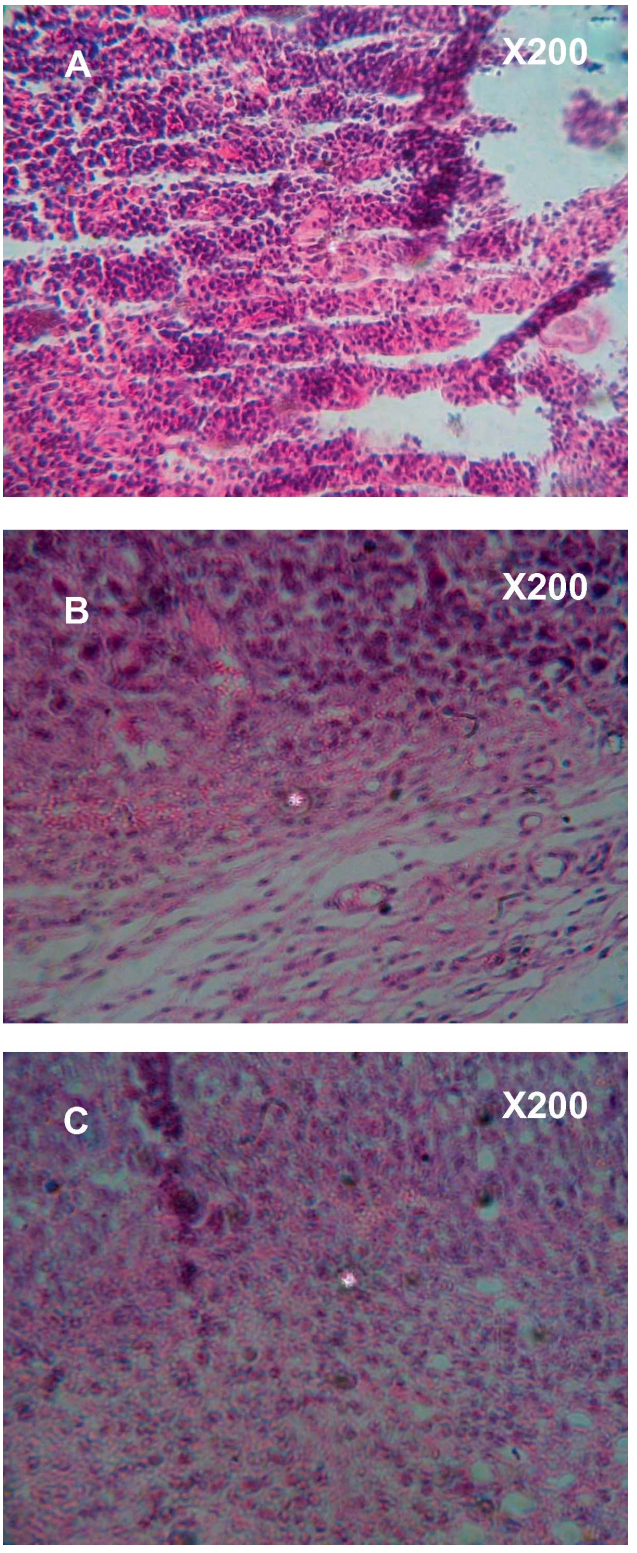

Figure 7. Histomorphology of the S-180 tumor cells treated with (A) NS group, NS-treated mice; (B) folate-PEG–SLLN group, folate-PEG–SLLN at a dose of 6 mg/kg paclitaxel-treated mice; and (C) paclitaxel injection group, paclitaxel injection at a dose of 6 mg/kg paclitaxel-treated mice (×200).

folate-PEG–SLLN for paclitaxel delivery. Furthermore, paclitaxel-loaded folate-PEG–SLLN avoided the use of polyoxyethylated castor oil in current clinical formulation that has limited stability and notable side effects, which exhibits a great advantage compared with Cremophor® EL for solubilization and formulation of paclitaxel. Therefore, folate-PEG–SLLN may be a promising new drug delivery system of paclitaxel for tumor therapy.

Acknowledgments

The authors are very grateful to the laboratory of Robert J. Lee in Ohio State University for the help in the preparation of folate-PEG–PE.

Declaration of interest

The authors report no conflicts of interest. The authors alone are responsible for the content and writing of this paper.

References

1. Horwitz SB. (1992). Mechanism of action of taxol. Trends Pharmacol Sci, 13:134–6.
2. Spencer CM, Faulds D. (1994). Paclitaxel. Drugs, 48:794–847.
3. Gregory RE, DeLisa AF. (1993). Paclitaxel: A new antineoplastic agent for refractory ovarian cancer. Clin Pharm, 12:401–15.
4. Yusuf RZ, Duan Z, Lamendola DE, Penson RT, Seiden MV. (2003). Paclitaxel resistance: Molecular mechanisms and pharmacologic manipulation. Curr Cancer Drug Targets, 3:1–19.
5. Lee J, Lee SC, Acharya G, Chang CJ, Park K. (2003). Hydrotropic solubilization of paclitaxel: Analysis of chemical structures for hydrotropic property. Pharm Res, 20:1022–30.
6. Henningsson A, Karlsson MO, Vigano L. (2001). Mechanism based pharmacokinetic model for paclitaxel. J Clin Oncol, 19:4065–73.
7. Szebeni J, Muggia FM, Alving CR. (1998). Complement activation by Cremophor EL as a possible contributor to hypersensitivity to paclitaxel: An in vitro study. J Natl Cancer Inst, 90:300–6.
8. Song D, Hsu LF, Au JLS. (1996). Binding of paclitaxel to plastic glass container and protein under in vitro conditions. J Pharm Sci, 85:29–31.
9. Paradis R, Page M. (1998). New active paclitaxel amino acids derivatives with improved water solubility. Anticancer Res, 18:2711–6.
10. Constantinides PP, Tustian A, Kessler DR. (2004). Tocol emulsion for drug solubilization and parenteral delivery. Adv Drug Deliv Rev, 56:1243–55.
11. Gradishar WJ, Tjulandin S, Davidson N, Shaw H, Desai N, Bhar P, et al. (2005). Phase III trial of nanoparticle albumin-bound paclitaxel compared with polyethylated castor oil-based paclitaxel in women with breast cancer. J Clin Oncol, 23:7794–803.
12. Gradishar WJ. (2006). Albumin-bound paclitaxel: A next-generation taxane. Expert Opin Pharmacother, 7(8):1041–53.
13. Müller RH, Mäder K, Gohla S. (2000). Solid lipid nanoparticles (SLN) for controlled drug delivery—a review of the state of the art. Eur J Pharm Biopharm, 50:161–77.
14. Chen DB, Yang TZ, Lu WL, Zhang Q. (2001). In vitro and in vivo study of two types of long-circulating solid lipid nanoparticless containing paclitaxel. Chem Pharm Bull, 49:1444–7.

15. Wissing SA, Kayser O, Müller RH. (2004). Solid lipid nanoparticless for parenteral drug delivery. Adv Drug Deliv Rev, 56:1257–72.
16. Jores K, Mehnert W, Drechsler M, Bunjes H, Johann C, Mäder K. (2004). Investigations on the structure of solid lipid nanoparticless (SLN) and oil-loaded solid lipid nanoparticless by photon correlation spectroscopy, field-flow fractionation and transmission electron microscopy. J Control Release, 95:217–27.
17. Torchilin VP, Trubetskoy VS. (1995). Which polymers can make nanoparticulate drug carriers long-circulating? Adv Drug Deliv Rev, 16:141–55.
18. Laginha K, Mumbengegwi D, Allen T. (2005). Liposomes targeted via two different antibodies: Assay, B-cell binding and cytotoxicity. Biochim Biophys Acta, 1711:25–32.
19. Campbell IG, Jones TA, Foulkes WD, Trowsdale J. (1991). Folate-binding protein is a marker for ovarian cancer. Cancer Res, 51:5329–38.
20. Garin-Chesa P, Campbell I, Saigo PE, Lewis JL, Old LJ, Rettig WJ. (1993). Trophoblast and ovarian cancer antigen LK26. Sensitivity and specificity in immunopathology and molecular identification as a folate-binding protein. Am J Pathol, 142:557–67.
21. Ross JF, Chaudhuri PK, Ratnam M. (1994). Differential regulation of folate receptor isoforms in normal and malignant tissues in vivo and in established cell lines. Cancer, 73:2432–43.
22. Parker N, Turk MJ, Westrick E, Lewis JD, Low PS, Leamon CP. (2005). Folate receptor expression in carcinomas and normal tissues determined by a quantitative radioligand binding assay. Anal Biochem, 338:284–93.
23. Leamon CP, Low PS. (1994). Selective targeting of malignant cells with cytotoxin-folate conjugates. J Drug Target, 2:101–12.
24. Lee RJ, Low PS. (1994). Delivery of liposomes into cultured KB cells via folate receptor-mediated endocytosis. J Biol Chem, 269:3198–204.
25. Lee RJ, Low PS. (1995). Folate-mediated tumor cell targeting of liposome entrapped doxorubicin in vitro. Biochim Biophys Acta, 1233:134–44.
26. Wang S, Lee RJ, Mathias CJ, Green MA, Low PS. (1996). Synthesis, purification, and tumor cell uptake of 67Ga-deferoxamine-folate, a potential radiopharmaceutical for tumor imaging. Bioconjug Chem, 7(1):56–62.
27. Li S, Deshmukh HM, Huang L. (1998). Folate-mediated targeting of antisense oligodeoxynucleotides to ovarian cancer cells. Pharm Res, 15:1540–5.
28. Shinoda T, Takagi A, Maeda A, Kagatani S, Konno Y, Hashida M. (1998). In vivo fate of folate-BSA in non-tumor- and tumor-bearing mice. J Pharm Sci, 87:1521–6.
29. Zhou W, Yuan X, Wilson A, Yang L, Mokotoff M, Pitt B, et al. (2002). Efficient intracellular delivery of oligonucleotides formulated in folate receptor-targeted lipid vesicles. Bioconjug Chem, 13:1220–5.
30. Ke CY, Mathias CJ, Green MA. (2003). The folate receptor as a molecular target for tumor-selective radionuclide delivery. Nucl Med Biol, 30:811–7.
31. Carlsson G, Gullberg B, Hafstrom L. (1983). Estimation of liver tumor volume using different formulas—an experimental study in rats. J Cancer Res Clin Oncol, 105:20–3.
32. Jung KO, Park SY, Park KY. (2006). Longer aging time increases the anticancer and antimetastatic properties of doenjang. Nutrition, 22:539–45.
33. Liu M, Xu W, Xu LJ, Zhong GR, Chen SL. (2005). Synthesis and biological evaluation of diethylenetriamine pentaacetic acid-polyethylene glycol-folate: A new folate-derived, 99mTc-based radiopharmaceutical. Bioconjug Chem, 16:1126–32.
34. Sahoo SK, Ma W, Labhasetwar V. (2004). Efficacy of transferrin-conjugated paclitaxel-loaded nanoparticless in a murine model of prostate cancer. Int J Cancer, 112:335–40.
35. Yang T, Choi MK, Cui FD, Kim JS, Chung SJ, Shim CK, et al. (2007). Preparation and evaluation of paclitaxel-loaded PEGylated immunoliposome. J Control Release, 120:169–77.
36. Lawrence JM, Petitti DB, Watkins M, Umekubo MA. (1999). Trends in serum folate after food fortification. Lancet, 354:915–6.
37. Yoo HS, Park TG. (2004). Folate receptor targeted biodegradable polymeric doxorubicin micelles. J Control Release, 96:273–83.
38. Zhang LK. (2005). Study on drug delivery system of folate-receptor-mediated mitoxantrone albumin nanoparticless targeting ovarian cancer cell. Doctoral dissertation. Sichuan University, China.